jove

Wide-Field, Real-Time Imaging of Local and Systemic Wound Signals in *Arabidopsis*

Takuya Uemura[1], **Jiaqi Wang**[1], **Yuri Aratani**[1], **Simon Gilroy**[2], **Masatsugu Toyota**[1,2]

[1] Department of Biochemistry and Molecular Biology, Saitama University [2] Department of Botany, University of Wisconsin

Corresponding Author

Masatsugu Toyota

mtoyota@mail.saitama-u.ac.jp

Citation

Uemura, T., Wang, J., Aratani, Y., Gilroy, S., Toyota, M. Wide-Field, Real-Time Imaging of Local and Systemic Wound Signals in *Arabidopsis*. *J. Vis. Exp.* (172), e62114, doi:10.3791/62114 (2021).

Date Published

June 4, 2021

DOI

10.3791/62114

URL

jove.com/video/62114

Abstract

Plants respond to mechanical stresses such as wounding and herbivory by inducing defense responses both in the damaged and in the distal undamaged parts. Upon wounding of a leaf, an increase in cytosolic calcium ion concentration (Ca^{2+} signal) occurs at the wound site. This signal is rapidly transmitted to undamaged leaves, where defense responses are activated. Our recent research revealed that glutamate leaking from the wounded cells of the leaf into the apoplast around them serves as a wound signal. This glutamate activates glutamate receptor-like Ca^{2+} permeable channels, which then leads to long-distance Ca^{2+} signal propagation throughout the plant. The spatial and temporal characteristics of these events can be captured with real-time imaging of living plants expressing genetically encoded fluorescent biosensors. Here we introduce a plant-wide, real-time imaging method to monitor the dynamics of both the Ca^{2+} signals and changes in apoplastic glutamate that occur in response to wounding. This approach uses a wide-field fluorescence microscope and transgenic *Arabidopsis* plants expressing Green Fluorescent Protein (GFP)-based Ca^{2+} and glutamate biosensors. In addition, we present methodology to easily elicit wound-induced, glutamate-triggered rapid and long-distance Ca^{2+} signal propagation. This protocol can also be applied to studies on other plant stresses to help investigate how plant systemic signaling might be involved in their signaling and response networks.

Introduction

Plants cannot escape from biotic stresses, e.g., insects feeding on them, so they have evolved sophisticated stress sensing and signal transduction systems to detect and then protect themselves from challenges such as herbivory[1]. Upon wounding or herbivore attack, plants initiate rapid defense responses including accumulation of the phytohormone jasmonic acid (JA) not only at the wounded site but also in undamaged distal organs[2]. This JA then both triggers defense responses in the directly damaged tissues and preemptively induces defenses in the undamaged parts of

the plant. In *Arabidopsis*, the accumulation of JA induced by wounding was detected in distal, intact leaves within just a few minutes of damage elsewhere in the plant suggesting that a rapid and long-distance signal is being transmitted from the wounded leaf[3]. Several candidates, such as Ca^{2+}, reactive oxygen species (ROS), and electrical signals, have been proposed to serve as these long-distance wound signals in plants[4,5].

Ca^{2+} is one of the most versatile and ubiquitous second messenger elements in eukaryotic organisms. In plants, caterpillar chewing and mechanical wounding cause drastic increases in the cytosolic Ca^{2+} concentration ($[Ca^{2+}]_{cyt}$) both in the wounded leaf and in unwounded distant leaves[6,7]. This systemic Ca^{2+} signal is received by intracellular Ca^{2+}-sensing proteins, which lead to the activation of downstream defense signaling pathways, including JA biosynthesis[8,9]. Despite numerous such reports supporting the importance of Ca^{2+} signals in plant wound responses, information on the spatial and temporal characteristics of Ca^{2+} signals induced by wounding is limited.

Real-time imaging using genetically encoded Ca^{2+} indicators is a powerful tool to monitor and quantify the spatial and temporal dynamics of Ca^{2+} signals. To date, versions of such sensors have been developed that enable the visualization of Ca^{2+} signals at the level of a single cell, to tissues, organs and even whole plants[10]. The first genetically encoded biosensor for Ca^{2+} used in plants was the bioluminescent protein aequorin derived from the jellyfish *Aequorea victoria*[11]. Although this chemiluminescent protein has been used to detect Ca^{2+} changes in response to various stresses in plants[12,13,14,15,16,17,18], it is not well-suited for real-time imaging due to the extremely low luminescent signal it produces. Förster Resonance Energy Transfer (FRET)-based Ca^{2+} indicators, such as the Yellow cameleons, have also been successfully used to investigate the dynamics of a range of Ca^{2+} signaling events in plants[19,20,21,22,23,24]. These sensors are compatible with imaging approaches and most commonly are composed of the Ca^{2+} binding protein calmodulin (CaM) and a CaM-binding peptide (M13) from a myosin light chain kinase, all fused between two fluorophore proteins, generally a Cyan Fluorescent Protein (CFP) and a Yellow Fluorescent Protein variant (YFP)[10]. Ca^{2+} binding to CaM promotes the interaction between CaM and M13 leading to a conformational change of the sensor. This change promotes energy transfer between the CFP and YFP, which increases the fluorescence intensity of the YFP while decreasing the fluorescence emission from the CFP. Monitoring this shift from CFP to YFP fluorescence then provides a measure of the increase in Ca^{2+} level. In addition to these FRET sensors, single fluorescent protein (FP)-based Ca^{2+} biosensors, such as GCaMP and R-GECO, are also compatible with plant imaging approaches and are widely used to study $[Ca^{2+}]_{cyt}$ changes due to their high sensitivity and ease of use[25,26,27,28,29,30]. GCaMPs contain a single circularly permutated (cp) GFP, again fused to CaM and the M13 peptide. The Ca^{2+}-dependent interaction between CaM and M13 causes a conformational change in the sensor that promotes a shift in the protonation state of the cpGFP, enhancing its fluorescent signal. Thus, as Ca^{2+} levels rise, the cpGFP signal increases.

To investigate the dynamics of Ca^{2+} signals generated in response to mechanical wounding or herbivore feeding, we have used transgenic *Arabidopsis thaliana* plants expressing a GCaMP variant, GCaMP3, and a wide-field fluorescence microscope[6]. This approach has succeeded in visualizing rapid transmission of a long-distance Ca^{2+} signal from the wound site on a leaf to the whole plant. Thus, an increase

in $[Ca^{2+}]_{cyt}$ was immediately detected at the wound site but this Ca^{2+} signal was then propagated to the neighboring leaves through the vasculature within a few minutes of wounding. Furthermore, we found that the transmission of this rapid systemic wound signal is abolished in *Arabidopsis* plants with mutations in two glutamate receptor-like genes, *Glutamate Receptor Like* (*GLR*), *GLR3.3,* and *GLR3.6*[6]. The GLRs appear to function as amino-acid gated Ca^{2+} channels involved in diverse physiological processes, including wound response[3], pollen tube growth[31], root development[32], cold response[33], and innate immunity[34]. Despite this well-understood, broad physiological function of the GLRs, information on their functional properties, such as their ligand specificity, ion selectivity, and subcellular localization, are limited[35]. However, recent studies reported that GLR3.3 and GLR3.6 are localized in the phloem and xylem, respectively. Plant GLRs have similarities to ionotropic glutamate receptors (iGluRs)[36] in mammals, which are activated by amino acids, such as glutamate, glycine, and D-serine in the mammalian nervous system[37]. Indeed, we demonstrated that the application of 100 mM glutamate, but not other amino acids, at the wound site induces a rapid, long-distance Ca^{2+} signal in *Arabidopsis*, indicating that extracellular glutamate likely acts as a wound signal in plants[6]. This response is abolished in the *glr3.3*/*glr3.6* mutant suggesting that glutamate may be acting through one or both of these receptor-like channels and indeed, AtGLR3.6 was recently shown to be gated by these levels of glutamate[38].

In plants, in addition to its role as a structural amino acid, glutamate has also been proposed as a key developmental regulator[39]; however, its spatial and temporal dynamics are poorly understood. Just as for Ca^{2+}, several genetically encoded indicators for glutamate have been developed to monitor the dynamics of this amino acid in living cells[40,41]. iGluSnFR is a GFP-based single-FP glutamate biosensor composed of cpGFP and a glutamate binding protein (GltI) from *Escherichia coli*[42,43]. The conformational change of iGluSnFR, that is induced by glutamate binding to GltI, results in an enhanced GFP fluorescence emission. To investigate whether extracellular glutamate acts as a signaling molecule in plant wound response, we connected the iGluSnFR sequence with the basic chitinase signal peptide secretion sequence (CHIB-iGluSnFR) to localize this biosensor in the apoplastic space[6]. This approach enabled imaging of any changes in the apoplastic glutamate concentration ($[Glu]_{apo}$) using transgenic *Arabidopsis* plants expressing this sensor. We detected rapid increases in the iGluSnFR signal at the wounding site. This data supports the idea that glutamate leaks out of the damaged cells/tissues to the apoplast upon wounding and acts as a damage signal activating the GLRs and leading to the long-distance Ca^{2+} signal in plants[6].

Here, we describe a plant-wide real-time imaging method using genetically encoded biosensors to monitor and analyze the dynamics of long-distance Ca^{2+} and extracellular glutamate signals in response to wounding[6]. The availability of wide-field fluorescence microscopy and transgenic plants expressing genetically encoded biosensors provides a powerful, yet easily implemented approach to detect rapidly transmitted long-distance signals, such as Ca^{2+} waves.

Protocol

1. Plant material preparation

1. In a 1.5 mL microtube, surface sterilize the seeds of *Arabidopsis thaliana* (Col-0 accession) plant expressing either GCaMP3 or CHIB-iGluSnFR by shaking with 20% (v/v) NaClO for 3 min and then wash 5 times with sterile distilled water.

NOTE: The transgenic lines of *Arabidopsis* expressing GCaMP3 or CHIB-iGluSnFR have been described previously[6].

2. In a sterile hood, sow 13 surface-sterilized seeds on a 10 cm square plastic Petri dish filled with 30 mL sterile (autoclaved) Murashige and Skoog (MS) medium [1x MS salts, 1% (w/v) sucrose, 0.01% (w/v) myoinositol, 0.05% (w/v) MES and 0.5% (w/v) gellan gum; pH 5.7 adjusted with 1N KOH]. Replace the lid and wrap with surgical tape.

3. After incubation in dark at 4 °C for 2 days, place the plates horizontally at 22 °C in a growth chamber under continuous light (90-100 µmol m^{-2} s^{-1}) for approximately 2 weeks before use. After 2 weeks, count the number of *Arabidopsis* leaves from oldest to youngest[44] (**Figure 1**). Wound responses preferentially move from the damaged leaf (n) to leaves numbered n ± 3 and n ± 5[6].

   NOTE: In this protocol, the Petri dish will be opened for imaging the wound and glutamate effects under a fluorescence microscope. Therefore, subsequent steps in this experiment should be conducted under temperature- and humidity-controlled room conditions. This is because Ca^{2+} signals are also elicited by changes in these environmental conditions. It is also known that the blue light, emitted from the microscope during recording for excitation of the biosensor protein's fluorescence, may elicit an increase of cytosolic Ca^{2+} concentration[45] and so the plant should be acclimated to the blue light irradiation for several minutes before beginning the experiment.

2. Chemical preparation

1. Dissolve L-Glutamate in a liquid growth medium [1/2x MS salts, 1% (w/v) sucrose and 0.05% (w/v) MES; pH 5.1 adjusted with 1N KOH] to make a 100 mM working solution.

   NOTE: Avoid use of salts of glutamate such as sodium glutamate to prevent potential cation-related effects on Ca^{2+} dynamics.

3. Microscope setting and conducting real-time imaging

1. Turn on the motorized fluorescence stereomicroscope equipped with a 1x objective lens (NA = 0.156) and a sCMOS camera (**Figure 2**) and configure the device settings to irradiate with a 470/40 nm excitation light and acquire an emission light passing through a 535/50 nm filter.

   NOTE: Any GFP-sensitive fluorescence microscope can be used to detect GCaMP3 and iGluSnFR signals in real-time, but a low power objective lens and highly sensitive camera with a wide sCMOS chip are recommended to acquire signals from the entire plant. The low power objective allows for imaging of an entire *Arabidopsis* plant's response and use of a highly sensitive camera permits the fast data acquisition needed to capture the rapid time course of the wound-triggered Ca^{2+} wave. For the fluorescence microscope used in this study, the maximum values of the field of view and temporal resolution are 3 cm x 3 cm and 30 frames per second (fps), respectively.

2. Remove the lid and place the dish under the objective lens.

3. Check the fluorescence signal from the plant and then wait for approximately 30 min in the dark until plants are adapted to the new environmental conditions. This adaptation step is required because changes in humidity elicit $[Ca^{2+}]_{cyt}$ elevation in plants that can interfere with any wound-related events.

4. Adjust the focus and magnification to see the whole plant in the field of view. In the current protocol, a 0.63x magnification was used.

5. Before starting real-time imaging, set up the acquisition parameters to detect the fluorescence signals using microscope imaging software. The settings for imaging in the current protocol are: exposure and interval times set to 1.8 s and 2 s (i.e., 0.5 fps), respectively. Set recording time to 11 min.

6. Image for 5 min prior to starting the experiment to acclimate the plant to the blue light irradiation from the microscope, then start recording by clicking on **Run Now**, or the equivalent command in the microscope software being used. To determine the average baseline fluorescence, record at least 10 frames (i.e., at least 20 s in the current protocol) before wounding or glutamate application (see Section 4).

    1. For real-time imaging of wound-induced $[Ca^{2+}]_{cyt}$ and $[Glu]_{apo}$ changes, cut the petiole or the middle region of leaf L1 with scissors (**Figure 3** and **Figure 4**).

    2. For real-time imaging of glutamate-triggered $[Ca^{2+}]_{cyt}$ changes, cut the edge (approximately 1 mm from the tip) of leaf 1 across the main vein with scissors. After at least 20 min recovery period, apply 10 µL of 100 mM glutamate to the leaf's cut surface (**Figure 5**).

        NOTE: This pre-cutting was necessary to allow glutamate access to the leaf apoplast in order to trigger responses. In addition, applying a drop of distilled water to the cut surface of leaf L1 was found to be critical to prevent the samples from desiccating during the recovery before applying glutamate.

7. After finishing the 11 min recording, save the data.

4. Data analysis

1. For fluorescence intensity analysis over time, define a region of interest (ROI) at the place where fluorescence intensity is to be analyzed (**Figure 6** and **Figure 7**). For the velocity calculation of the Ca^{2+} wave, define 2 ROIs (ROI1 and ROI2) for analysis. In the imaging software, click on **Time Measurement | Define | Circle**. Measure the distance between ROI1 and ROI2 by clicking on **Annotations and Measurement | Length | Simple Line** (**Figure 6**).

2. Measure the raw fluorescence values (F) in each ROI over time by clicking on **Measure**. Export raw data to a spreadsheet software to convert the fluorescence signal into numbers at each time point by clicking on **All to Excel | Export**.

3. Determine the baseline fluorescence value, which is defined as F_0, by calculating the average of F over the first 10 frames (i.e., prior to treatment) in the recorded data.

4. Normalize the F data (by calculating $\Delta F/F$) using the equation $\Delta F/F = (F-F_0)/F_0$, where ΔF is the time-dependent change in fluorescence.

5. For Ca^{2+} wave velocity wave analysis, define a significant signal rise point above the pre-stimulated values as representing detection of a Ca^{2+} increase in each ROI (t_1 and t_2) using the criterion of a rise to 2× the standard deviation (2x SD) that is calculated from the F_0 data using statistical software. 95% of the F_0 data falls within 2x SD from the mean, indicating that a rise in signal above this level by chance is ≤5%. Calculate the time difference of the Ca^{2+} increase between ROI1 and ROI2 [t_2- t_1 time-lag (Δt)] and measure the distance between ROI1 and ROI2, then determine the velocities of any Ca^{2+} wave.

Representative Results

Signal propagation of $[Ca^{2+}]_{cyt}$ and $[Glu]_{apo}$ in response to wounding is presented in **Figure 3**, **Figure 4**, **Movie S1**, and **Movie S2**. Cutting the petiole of the leaf 1 in plants expressing GCaMP3 (at 0 s) led to a significant increase in $[Ca^{2+}]_{cyt}$ that was rapidly induced locally through the vasculature (at 40 s) (**Figure 3** and **Movie S1**). Subsequently, the signal was rapidly propagated to neighboring leaves (leaf 3 and 6) within a few minutes (at 80 s) (**Figure 3** and **Movie S1**).

Upon cutting leaf 1 in plants expressing CHIB-iGluSnFR, a rapid $[Glu]_{apo}$ increase was observed around the cut region (at 2 s). This signal was propagated through the vasculature locally within a few minutes (at 160 s) but was not observed in systemic leaves (**Figure 4** and **Movie S2**).

For the real-time imaging of Ca^{2+} signal propagation triggered by the application of glutamate, the edge (approximately 1 mm from the tip) of leaf 1 in plants expressing GCaMP3 was cut as shown in **Figure 5A** and **Movie S3**. Cutting the edge of leaf 1 caused a local $[Ca^{2+}]_{cyt}$ increase (at 40 s) but this signal disappeared within a few minutes (at 124 s). After waiting for approximately 10 min for the plant to recover, 10 µL of 100 mM glutamate was applied to the cut surface of leaf 1, which caused a rapid, significant increase of $[Ca^{2+}]_{cyt}$ locally (at 56 s) and signal propagation to distal leaves (at 104 s) (**Figure 5B** and **Movie S4**).

To measure the changes in $[Ca^{2+}]_{cyt}$ induced by wounding in the systemic leaf, two ROIs (ROI1 and ROI2) were set at the base region and tip of leaf 6 in plants expressing GCaMP3 as shown in **Figure 6A**. The time course change of GCaMP3 signal intensity in ROI1 and ROI2 upon cutting the petiole of leaf 1 was measured (**Figure 6B**). A significant increase of $[Ca^{2+}]_{cyt}$ at ROI1 was detected earlier than that of ROI2 (**Figure 6B**). $[Ca^{2+}]_{cyt}$ peaked at approximately 100 s after wounding, lasted for over 10 min, and exhibited two phases (**Figure 6B**).

To determine the velocities of the Ca^{2+} wave upon mechanical wounding, the timepoint of a significant signal rise above the pre-stimulated values in ROI1 and ROI2 was determined (time-lag; see Section 4) (**Figure 6C**). Because the distance between ROI1 and ROI2 was 2.7 mm in this case (**Figure 6A**), the Ca^{2+} signal velocity in leaf 6 was calculated as 0.15 mm/s. To measure the $[Glu]_{apo}$ changes in response to the mechanical damage, ROI1 was set in the vicinity of cutting site of the leaf marked as L1 as shown in **Figure 7A**. $[Glu]_{apo}$ signature at ROI1 has exhibited a single peak at approximately 100 s upon wounding (**Figure 7B**).

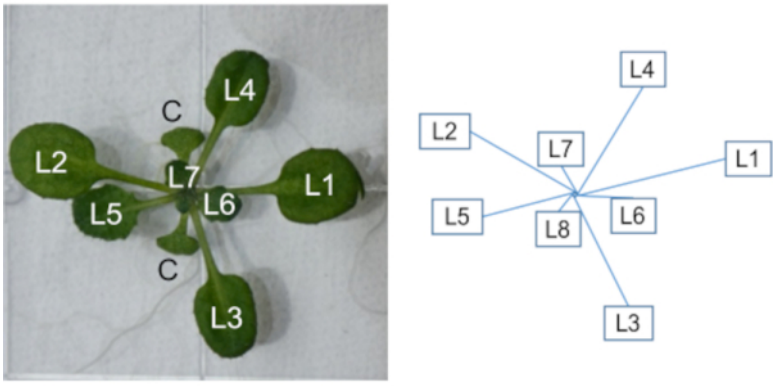

Figure 1: Numbering of *Arabidopsis* rosette leaves. *Arabidopsis* leaves are numbered from oldest to youngest (left panel). A schematic diagram of the leaves' position is indicated in the right panel. L: leaf, C: cotyledons. Please click here to view a larger version of this figure.

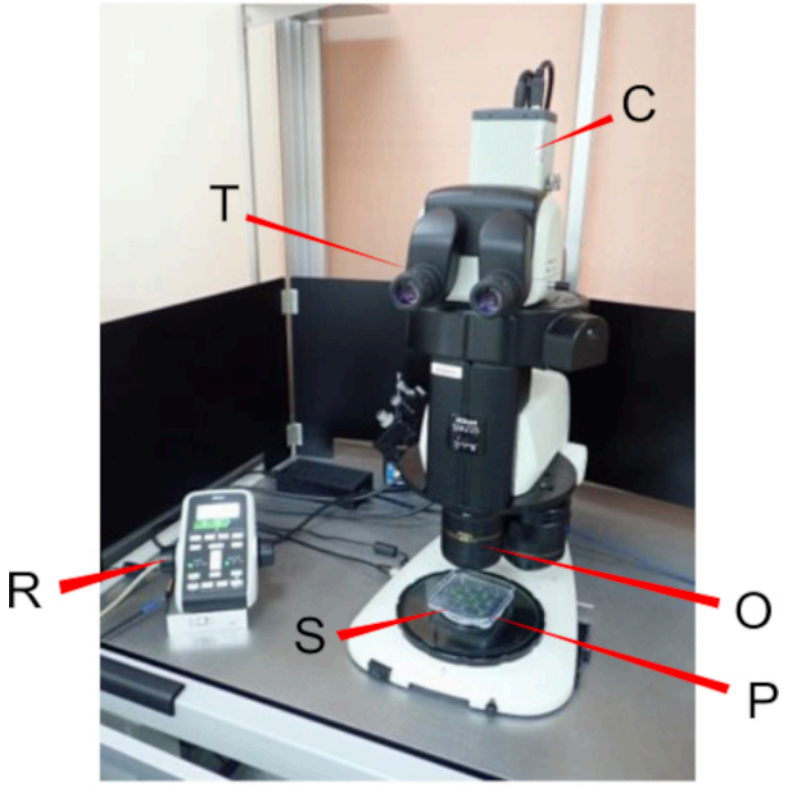

Figure 2: A fluorescence microscope used in this study. $[Ca^{2+}]_{cyt}$ and $[Glu]_{apo}$ dynamics were imaged with a wide-field fluorescence stereomicroscope. R: Remote controller, O: 1x objective lens, C: sCMOS camera, T: Trinocular tilting tube, S: Stage, P: Plant material. Please click here to view a larger version of this figure.

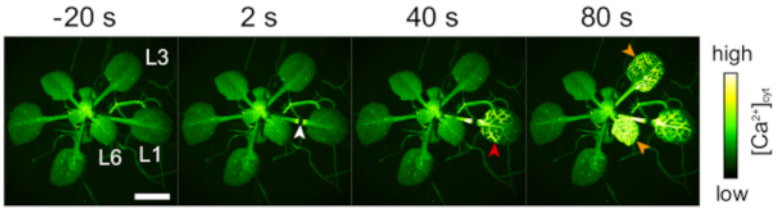

Figure 3: Wound-induced long-distance Ca^{2+} signal transmission. Cutting the petiole (white arrow, 0 s) of leaf 1 (L1) in plant expressing GCaMP3 triggered a local $[Ca^{2+}]_{cyt}$ increase (red arrow, 40 s) that was transmitted to systemic leaves [leaf 3 (L3) and leaf 6 (L6)] (orange arrows, 80 s). Scale bar, 5 mm. Please click here to view a larger version of this figure.

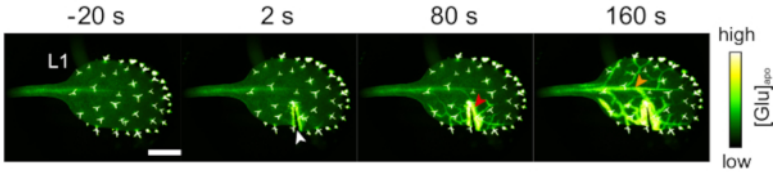

Figure 4: Wound-triggered $[Glu]_{apo}$ elevation. Cutting the leaf 1 (L1) (white arrow, 0 s) in plants expressing CHIB-iGluSnFR caused a rapid elevation of $[Glu]_{apo}$ (red arrow, 80 s) that propagated through the vasculature (orange arrow, 160 s). Scale bar, 2 mm. Please click here to view a larger version of this figure.

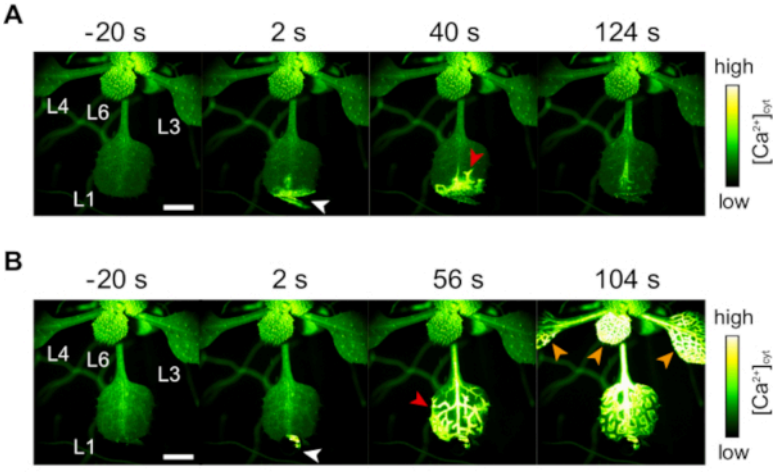

Figure 5: Glutamate-triggered long-distance Ca^{2+} signal transmission. (**A**) Cutting the edge (approximately 1 mm from the tip) of leaf 1 (L1) in plants expressing GCaMP3 (white arrow, 0 s) caused a $[Ca^{2+}]_{cyt}$ increase (red arrow, 40 s). (**B**) Application of 100 mM glutamate to the cut surface of L1 (white arrow, 0 s) caused a local $[Ca^{2+}]_{cyt}$ increase (red arrow, 56 s) that rapidly propagated to distal leaves [e.g., leaf 3 (L3), leaf 4 (L4), and leaf 6 (L6)] (orange arrows, 104 s). Scale bars, 5 mm. Please click here to view a larger version of this figure.

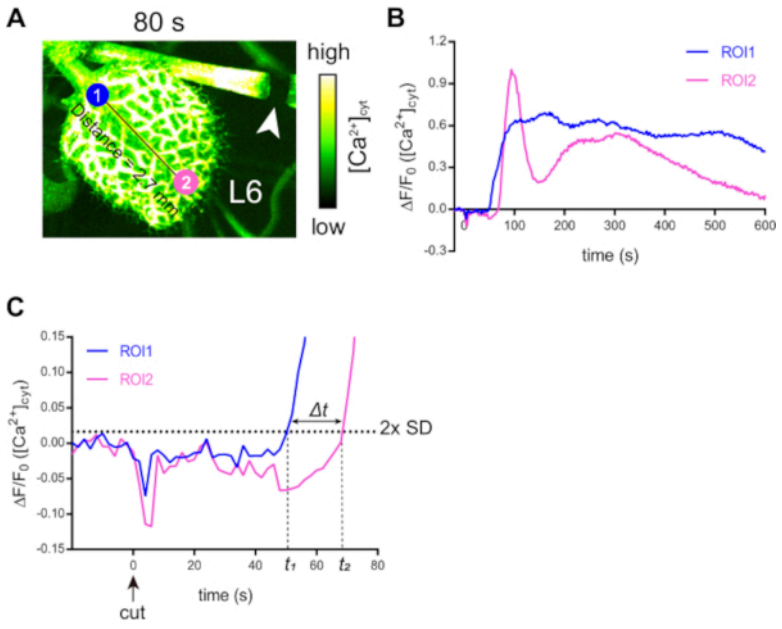

Figure 6: $[Ca^{2+}]_{cyt}$ signature in systemic leaves in response to mechanical wounding. (**A**) An expanded image of leaf 6 (L6) in plants expressing GCaMP3 is shown in **Figure 3**. ROI1 (blue circle) and ROI2 (pink circle) were set at the base and tip region, respectively. White arrow indicates the cut site of leaf 1's petiole (L1). In this case, the distance between ROI1 and ROI2 was 2.7 mm. (**B**) Quantification of $[Ca^{2+}]_{cyt}$ signatures in ROI1 and ROI2. Fluorescence intensity changes were analyzed using imaging software. (**C**) An expanded trace of data in (B) between 0 s and 80 s. Detection points of a Ca^{2+} increase in ROI1 and ROI2 were defined as t_1 and t_2, respectively, using as a criterion a rise to 2x the standard deviation of the prestimulation values (2x SD, dotted line). The value of t_2 - t_1 was defined as time-lag (Δt) in the current protocol. Black arrow indicates the cut time. Please click here to view a larger version of this figure.

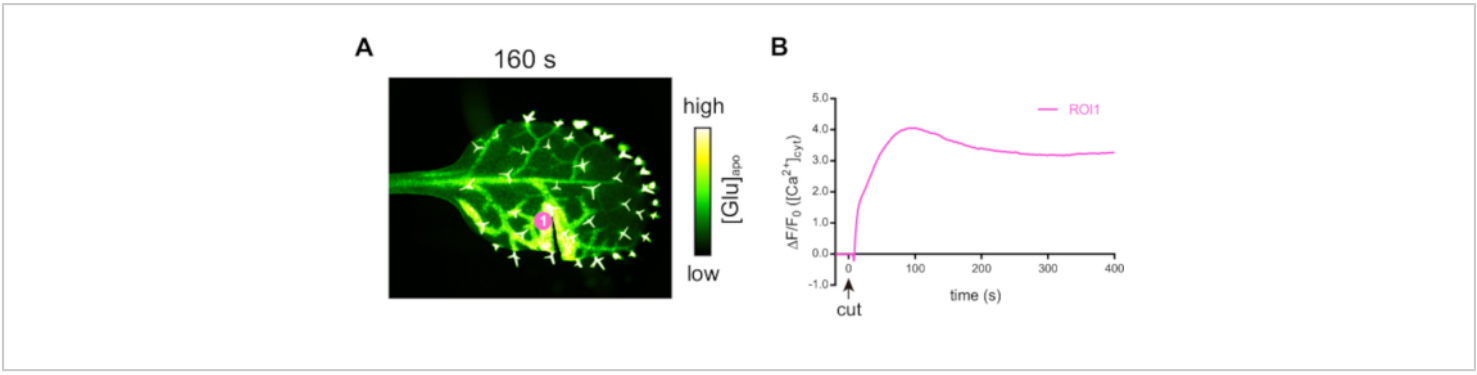

Figure 7: $[Glu]_{apo}$ signature in response to mechanical wounding. (**A**) An expanded image of leaf 1 (L1) in plants expressing CHIB-iGluSnFR is shown in **Figure 4**. ROI1 was set in the vicinity of the cut site. White arrow indicates the cut region. (**B**) Quantitation of $[Glu]_{apo}$ signature in ROI1 is monitored using imaging software. Black arrow indicates the cut time. Please click here to view a larger version of this figure.

Movie S1: Long-distance Ca^{2+} transmission after mechanical wounding. Mechanical wounding at the petiole of leaf 1 (L1) caused a $[Ca^{2+}]_{cyt}$ increase transmitted to distal leaves [e.g., leaf 3 (L3) and leaf 6 (L6)]. Please click here to download this movie.

Movie S2: Elevation of the apoplastic glutamate levels in response to cutting. Mechanical wounding of the leaf 1 (L1) caused an immediate increase in $[Glu]_{apo}$. Please click here to download this movie.

Movie S3: Elevation of $[Ca^{2+}]_{cyt}$ levels in response to cutting. Mechanical wounding at the edge of leaf 1 (L1) caused an immediate, local $[Ca^{2+}]_{cyt}$ elevation. Please click here to download this movie.

Movie S4: Application of glutamate triggers systemic $[Ca^{2+}]_{cyt}$ increases. Application of 100 mM glutamate triggered Ca^{2+} transmission to systemic leaves [e.g., leaf 3 (L3), leaf 4 (L4) and leaf 6 (L6)]. Please click here to download this movie.

Discussion

Systemic signaling is important for plants to respond to localized external environmental stimuli and then to maintain their homeostasis at a whole plant level. Although they are not equipped with an advanced nervous system like animals, they employ rapid communication both within and between organs based on factors such as mobile electrical (and possibly hydraulic) signals and propagating waves of ROS and Ca^{2+} [46,47]. The protocol described above allows plant-wide, real-time imaging of the activity of this signaling system through monitoring the dynamics of Ca^{2+} and apoplastic glutamate in response to wounding. This method provides a robust tool to understand rapid and long-distance signals in plants combining high spatiotemporal resolution and ease of use. This protocol also offers the potential to provide new physiological insights into the molecular mechanisms underlying long-distance wound signaling through, e.g., using mutants that are defective in putative elements of the rapid signaling system or exploration of the effects of pharmacological reagents such as Ca^{2+} channel blockers

(e.g., $LaCl_3$) or inhibitors of other potentially key signaling activities[6].

One important advantage of the biosensor imaging method described is the use of single-FP biosensors with high fluorescent yield, greatly simplifying both the required equipment to make these measurements and their in planta use. Thus, fluorescence-based genetically encoded indicators are divided into two classes: 1) intensity-based single-FP biosensors and 2) ratiometric FRET-based biosensors[10]. Although ratiometric FRET-based sensors are quantitatively accurate, intensity-based Ca^{2+} indicators, including the GCaMP3 and iGluSnFR used here, provide both higher temporal resolution and ease of use due to their generally brighter Ca^{2+}-responsive signal and their simpler microscope requirements[10]. For example, the red-fluorescent protein-based single-FP Ca^{2+} indicator R-GECO1 was reported to show a much greater signal change in response to extracellular ATP and the plant defense elicitors flg22 and chitin, when compared to the ratiometric YC3.6 biosensor[27]. For analysis of ratiometric FRET-based sensors, it is also necessary to use a specialized microscope with multiple filters to collect data at two wavelengths, whereas single-FP-based biosensors require the device to collect the data at only one wavelength, a capability found in all standard fluorescence microscopes[10]. However, it is important to note that there are some disadvantages of using single-FP biosensors. These intensity-based, single-FP biosensors are not preferred for quantifying absolute concentration changes or for long-term imaging over many hours or days. This limitation is because in addition to, e.g., Ca^{2+} level for GCaMP3, the signal intensity from these single-FP biosensors is thought to be affected by other factors such as the sensor expression level or parameters such as cellular pH that may change over time.

To date, many new variants of these genetically encoded indicators have been engineered to improve the signal to noise ratio, dynamic range, kinetics, and sensor stability. For example, after Nakai et al.[26] developed the first GCaMP, various successive variants, such as the GECOs have been generated by a combination of mutagenesis and careful characterization[48,49,50]. The dynamic range of G-GECO (Green-GECO) was reported to be approximately two-fold larger than that of GCaMP3[28]. Furthermore, the replacement with different fluorescent proteins in these indicators led to the generation of GECO variants with different emission spectra, such as B-GECO (Blue-GECO) and R-GECO (Red-GECO), which enables the use of these indicators alongside other GFP spectral variants in multi-color imaging applications[28]. Similarly, GCaMP has continued to be developed and improved with a series of sensors enhanced for speed of response and amplitude of signal now being available[50]. For monitoring glutamate dynamics, other than iGluSnFR, a series of FRET-based glutamate biosensors, the FLuorescent Indicator Proteins for Glutamate (FLIPE) have been developed[40]. FLIPE is composed of CFP and YFP that are linked via the glutamate binding protein ybeJ taken from *E. coli*. Upon glutamate binding to ybeJ, a glutamate concentration-dependent decrease of FRET efficiency is observed. Therefore, for both Ca^{2+} and glutamate there are multiple single-FP and ratiometric sensors available. Researchers should consider the appropriate biosensor to detect signal dynamics depending on the experimental design and requirements for measurement factors such as high signal:noise (single-FP sensors) versus a need for highly accurate quantitation (where FRET sensors excel).

The wide-field, single-FP imaging method described here for wounding should also be useful when applied to other stress systemic signaling processes. Despite the presence of numerous reports that suggest a crucial role of long-distance Ca^{2+} signaling in various stress responses, such as herbivore attack[6,51,52], salt[20], and drought[53], only a few studies have provided the spatiotemporal information related to rapid long-distance Ca^{2+} signals induced by these stress responses[6,7,20,52]. The use of a wide-field fluorescence microscope in this protocol also allows the real-time observation of mobile signal dynamics not only in leaf-to-leaf communication but also root-to-shoot communication as recently shown[38]. Although we have focused on protocols for *Arabidopsis*, this plant-wide real-time imaging method also provides a robust tool to understand the spatial and temporal characteristics of systemic Ca^{2+} signaling in both biotic and abiotic stress responses in other plant species such as tobacco[30].

Disclosures

The authors do not have any conflicts of interest.

Acknowledgments

This work was supported by grants from the Japan Society for the Promotion of Science (17H05007 and 18H05491) to MT, the National Science Foundation (IOS1557899 and MCB2016177) and the National Aeronautics and Space Administration (NNX14AT25G and 80NSSC19K0126) to SG.

References

1. Wu, J., Baldwin, I. T. Herbivory-induced signalling in plants: perception and action. *Plant, Cell & Environment.* **32** (9), 1161-1174 (2009).
2. Howe, G. A., Major, I. T., Koo, A. J. Modularity in Jasmonate Signaling for Multistress Resilience. *Annual Review of Plant Biology.* **69** (1), 387-415 (2018).
3. Mousavi, S. A. R., Chauvin, A., Pascaud, F., Kellenberger, S., Farmer, E. E. GLUTAMATE RECEPTOR-LIKE genes mediate leaf-to-leaf wound signalling. *Nature.* **500** (7463), 422-426 (2013).
4. Gilroy, S. et al. ROS, Calcium, and Electric Signals: Key Mediators of Rapid Systemic Signaling in Plants. *Plant Physiology.* **171** (3), 1606-1615 (2016).
5. Choi, W.-G., Hilleary, R., Swanson, S. J., Kim, S.-H., & Gilroy, S. Rapid, long-distance electrical and calcium signaling in plants. *Annual Review of Plant Biology.* **67** (1), 287-307 (2016).
6. Toyota, M. et al. Glutamate triggers long-distance, calcium-based plant defense signaling. *Science.* **361** (6407), 1112-1115 (2018).
7. Nguyen, C. T., Kurenda, A., Stolz, S., Chételat, A., Farmer, E. E. Identification of cell populations necessary for leaf-to-leaf electrical signaling in a wounded plant. *Proceedings of the National Academy of Sciences of the United States of America.* **115** (40), 10178-10183 (2018).
8. Lecourieux, D., Ranjeva, R., Pugin, A. Calcium in plant defence-signalling pathways. *New Phytologist.* **171** (2), 249-269 (2006).
9. Farmer, E. E., Gao, Y.-Q., Lenzoni, G., Wolfender, J.-L., Wu, Q. Wound- and mechanostimulated electrical signals control hormone responses. *New Phytologist.* **227** (4), 1037-1050 (2020).
10. Palmer, A. E., Qin, Y., Park, J. G., McCombs, J. E. Design and application of genetically encoded biosensors. *Trends in Biotechnology.* **29** (3), 144-152 (2011).

11. Ridgway, E. B., Ashley, C. C. Calcium transients in single muscle fibers. *Biochemical and Biophysical Research Communications.* **29** (2), 229-234 (1967).

12. Kiegle, E., Moore, C. A., Haseloff, J., Tester, M. A., Knight, M. R. Cell-type-specific calcium responses to drought, salt and cold in the *Arabidopsis* root. *The Plant Journal.* **23** (2), 267-278 (2000).

13. Zhu, X., Feng, Y., Liang, G., Liu, N., Zhu, J.-K. Aequorin-based luminescence imaging reveals stimulus- and tissue-specific Ca^{2+} dynamics in *Arabidopsis* plants. *Molecular Plant.* **6** (2), 444-455 (2013).

14. Kwaaitaal, M., Huisman, R., Maintz, J., Reinstädler, A., Panstruga, R. Ionotropic glutamate receptor (iGluR)-like channels mediate MAMP-induced calcium influx in **Arabidopsis thaliana**. *Biochemical Journal.* **440** (3), 355-373 (2011).

15. Vatsa, P. et al. Involvement of putative glutamate receptors in plant defence signaling and NO production. *Biochimie.* **93** (12), 2095-2101 (2011).

16. Toyota, M., Furuichi, T., Sokabe, M., Tatsumi, H. Analyses of a gravistimulation-specific Ca^{2+} signature in Arabidopsis using parabolic flights. *Plant Physiology.* **163** (2), 543-554 (2013).

17. Toyota, M. Hypergravity stimulation induces changes in intracellular calcium concentration in *Arabidopsis* seedlings. *Advances in Space Research.* **39**, 1190-1197 (2007).

18. Stephan, A. B., Kunz, H.-H., Yang, E., Schroeder, J. I. Rapid hyperosmotic-induced Ca^{2+} responses in *Arabidopsis thaliana* exhibit sensory potentiation and involvement of plastidial KEA transporters. *Proceedings of the National Academy of Sciences of the United States of America.* **113** (35), E5242-E5249 (2016).

19. Nagai, T., Yamada, S., Tominaga, T., Ichikawa, M., Miyawaki, A. Expanded dynamic range of fluorescent indicators for Ca^{2+} by circularly permuted yellow fluorescent proteins. *Proceedings of the National Academy of Sciences of the United States of America.* **101** (29), 10554-10559 (2004).

20. Choi, W.-G., Toyota, M., Kim, S.-H., Hilleary, R., Gilroy, S. Salt stress-induced Ca^{2+} waves are associated with rapid, long-distance root-to-shoot signaling in plants. *Proceedings of the National Academy of Sciences of the United States of America.* **111** (17), 6497-6502 (2014).

21. Evans, M. J., Choi, W.-G., Gilroy, S., Morris, R. J. A ROS-assisted calcium wave dependent on the AtRBOHD NADPH oxidase and TPC1 cation channel propagates the systemic response to salt stress. *Plant Physiology.* **171** (3), 1771-1784 (2016).

22. Hilleary, R. et al. Tonoplast-localized Ca^{2+} pumps regulate Ca^{2+} signals during pattern-triggered immunity in *Arabidopsis thaliana. Proceedings of the National Academy of Sciences of the United States of America.* **117** (31), 18849-18857 (2020).

23. Lenglet, A. et al. Control of basal jasmonate signalling and defence through modulation of intracellular cation flux capacity. *New Phytologist.* **216** (4), 1161-1169 (2017).

24. Choi, W.-G., Swanson, S. J., Gilroy, S. High-resolution imaging of Ca^{2+}, redox status, ROS and pH using GFP biosensors. *The Plant Journal.* **70** (1), 118-128 (2012).

25. Nagai, T., Sawano, A., Park, E. S., Miyawaki, A. Circularly permuted green fluorescent proteins

engineered to sense Ca^{2+}. *Proceedings of the National Academy of Sciences of the United States of America.* **98** (6), 3197-3202 (2001).

26. Nakai, J., Ohkura, M., Imoto, K. A high signal-to-noise Ca^{2+} probe composed of a single green fluorescent protein. *Nature Biotechnology.* **19** (2), 137-141 (2001).
27. Keinath, N. F. et al. Live cell imaging with R-GECO1 sheds light on flg22- and Chitin-induced transient $[Ca^{2+}]_{cyt}$ patterns in Arabidopsis. *Molecular Plant.* **8** (8), 1188-1200 (2015).
28. Zhao, Y. et al. An expanded palette of genetically encoded Ca^{2+} indicators. *Science.* **333** (6051), 1888-1891 (2011).
29. Vincent, T. R. et al. Real-time in vivo recording of Arabidopsis calcium signals during insect feeding using a fluorescent biosensor. *JoVE.* (126), e56142 (2017).
30. DeFalco, T. A. et al. Using GCaMP3 to study Ca^{2+} signaling in nicotiana species. *Plant and Cell Physiology.* **58** (7), 1173-1184 (2017).
31. Michard, E. et al. Glutamate receptor-like genes form Ca^{2+} channels in pollen tubes and are regulated by Pistil D-Serine. *Science.* **332** (6028), 434-437 (2011).
32. Singh, S. K., Chien, C.-T., Chang, I.-F. The Arabidopsis glutamate receptor-like gene GLR3.6 controls root development by repressing the Kip-related protein gene KRP4. *Journal of Experimental Botany.* **67** (6), 1853-1869 (2016).
33. Li, H. et al. Tomato GLR3.3 and GLR3.5 mediate cold acclimation-induced chilling tolerance by regulating apoplastic H_2O_2 production and redox homeostasis. *Plant, Cell & Environment.* **42** (12), 3326-3339 (2019).
34. Li, F. et al. Glutamate receptor-like channel3.3 is involved in mediating glutathione-triggered cytosolic calcium transients, transcriptional changes, and innate immunity responses in *Arabidopsis*. *Plant Physiology.* **162** (3), 1497-1509 (2013).
35. Wudick, M. M., Michard, E., Oliveira Nunes, C., Feijó, J. A. Comparing plant and animal glutamate receptors: common traits but different fates? *Journal of Experimental Botany.* **69** (17), 4151-4163 (2018).
36. De Bortoli, S., Teardo, E., Szabò, I., Morosinotto, T., Alboresi, A. Evolutionary insight into the ionotropic glutamate receptor superfamily of photosynthetic organisms. *Biophysical Chemistry.* **218**, 14-26 (2016).
37. Janovjak, H., Sandoz, G., Isacoff, E. Y. A modern ionotropic glutamate receptor with a K^+ selectivity signature sequence. *Nature Communications.* **2** (1), 232 (2011).
38. Shao, Q., Gao, Q., Lhamo, D., Zhang, H., Luan, S. Two glutamate- and pH-regulated Ca^{2+} channels are required for systemic wound signaling in *Arabidopsis. Science Signaling.* **13** (640), eaba1453 (2020).
39. Forde, B. G., Lea, P. J. Glutamate in plants: metabolism, regulation, and signalling. *Journal of Experimental Botany.* **58** (9), 2339-2358 (2007).
40. Okumoto, S. et al. Detection of glutamate release from neurons by genetically encoded surface-displayed FRET nanosensors. *Proceedings of the National Academy of Sciences of the United States of America.* **102** (24), 8740-8745 (2005).
41. Hires, S. A., Zhu, Y., Tsien, R. Y. Optical measurement of synaptic glutamate spillover and reuptake by linker optimized glutamate-sensitive fluorescent reporters.

Proceedings of the National Academy of Sciences of the United States of America. **105** (11), 4411-4416 (2008).

42. Marvin, J. S. et al. An optimized fluorescent probe for visualizing glutamate neurotransmission. *Nature Methods.* **10** (2), 162-170 (2013).
43. Marvin, J. S. et al. Stability, affinity, and chromatic variants of the glutamate sensor iGluSnFR. *Nature Methods.* **15** (11), 936-939 (2018).
44. Farmer, E., Mousavi, S. A. R., Lenglet, A. Leaf numbering for experiments on long distance signalling in Arabidopsis. *Protocol Exchange*: *Preprint server.* (2013).
45. Harada, A., Shimazaki, K.-i. Phototropins and blue light-dependent calcium signaling in higher plants. *Photochemistry and Photobiology.* **83** (1), 102-111 (2007).
46. Huber, A. E., Bauerle, T. L. Long-distance plant signaling pathways in response to multiple stressors: the gap in knowledge. *Journal of Experimental Botany.* **67** (7), 2063-2079 (2016).
47. Choi, W.-G. et al. Orchestrating rapid long-distance signaling in plants with Ca^{2+}, ROS and electrical signals. *The Plant Journal.* **90** (4), 698-707 (2017).
48. Tallini, Y. N. et al. Imaging cellular signals in the heart *in vivo*: cardiac expression of the high-signal Ca^{2+} indicator GCaMP2. *Proceedings of the National Academy of Sciences of the United States of America.* **103** (12), 4753-4758 (2006).
49. Tian, L. et al. Imaging neural activity in worms, flies and mice with improved GCaMP calcium indicators. *Nature Methods.* **6** (12), 875-881 (2009).
50. Chen, T.-W. et al. Ultrasensitive fluorescent proteins for imaging neuronal activity. *Nature.* **499** (7458), 295-300 (2013).
51. Vincent, T. R. *et al.* Interplay of plasma membrane and vacuolar ion channels, together with BAK1, elicits rapid cytosolic calcium elevations in Arabidopsis during aphid feeding. *The Plant Cell.* **29** (6), 1460-1479 (2017).
52. Meena, M. K. et al. The Ca^{2+} channel CNGC19 regulates Arabidopsis defense against spodoptera herbivory. *The Plant Cell.* **31** (7), 1539-1562 (2019).
53. Cheong, Y. H. et al. CBL1, a calcium sensor that differentially regulates salt, drought, and cold responses in Arabidopsis. *The Plant Cell.* **15** (8), 1833-1845 (2003).